Electron Transfer between Q A and Q B in Photosystem II Is Thermodynamically Perturbed in Phototolerant Mutants of Synechocystis sp . PCC 6803

ARTICLE *in* BIOCHEMISTRY · FEBRUARY 1999

Impact Factor: 3.02 · DOI: 10.1021/bi981217x · Source: PubMed

4 AUTHORS, INCLUDING:

Jun Minagawa
National Institute for Basic Biology
62 PUBLICATIONS **2,544** CITATIONS
SEE PROFILE

Kimiyuki Satoh
Okayama University
141 PUBLICATIONS **5,463** CITATIONS
SEE PROFILE

Electron Transfer between Q_A and Q_B in Photosystem II Is Thermodynamically Perturbed in Phototolerant Mutants of *Synechocystis sp*. PCC 6803

Jun Minagawa,*,‡ Yoshihiro Narusaka,§,|| Yorinao Inoue,‡ and Kimiyuki Satoh§

Photosynthesis Research Laboratory, The Institute of Physical and Chemical Research (RIKEN), 2-1 Hirosawa, Wako, Saitama 351-0198, Japan, and Department of Biology, Faculty of Science, Okayama University, 3-1-1 Tsushimanaka, Okayama 700-8530, Japan

Received May 22, 1998; Revised Manuscript Received September 17, 1998

ABSTRACT: Several random mutations have been generated in the *psbA2* gene of *Synechocystis* sp. PCC 6803 [Narusaka, Y., Murakami, A., Saeki, J., Kobayashi, H., and Satoh, K. (1996) *Plant Sci. 115*, 261−266]. The phototolerant mutant (I6) carrying all the amino acid substitutions in the lumenal side of D1 protein (S322I, I326F, and F328S) and a site-directed mutant of the same phenotype (NDFS) substituted in the stromal side of the protein (N234D and F260S) were characterized by thermoluminescence measurements. We observed (1) no significant differences in their growth rates at either low or high light irradiance, (2) a downshifted B-band in the NDFS mutant, (3) an upshifted Q-band in the I6 mutant, and (4) a damped period four oscillation of thermoluminescence in the B-band of both mutants. By examining the possible implications of these results on the redox properties of the PS II components in the mutants, we concluded that equilibrium constants for sharing an electron between the primary (Q_A) and secondary acceptor plastoquinones (Q_B) are decreased in both mutants.

The reaction center of photosystem II (PS II)[1] consists of two structurally similar proteins, D1 and D2, as well as cytochrome b_{559} and the *psbI* gene product (for a recent review, see ref *1*). The D1 and D2 polypeptides exist as heterodimers within the thylakoid membrane and bind the key components that mediate primary charge separation and water oxidation. The D1 protein of PS II reaction center plays a central role in the energy transformation and is the most irradiation-sensitive component. Although light is an invaluable source of energy, photosynthetic organisms suffer unavoidable damage from high light intensity. Extensive studies have been completed, especially in the past decade, investigating the molecular mechanisms of the photodamage (photoinhibition) and exploring the intrinsic strategy of photosynthetic organisms to cope with high light (*2*).

Recently, 18 distinct mutants were generated by in vitro random mutagenesis of the *psbA2* gene in *Synechocystis* sp. PCC 6803, which form blue-green colonies under high light conditions (*3*−*5*). Mutational effects on the D1 protein enable these phototolerant mutants to maintain the blue-green color under high light conditions. These mutants have been characterized in order to elucidate a mechanism that enables this organism to cope with high light irradiation (*4*). In the present paper, the word phototolerance will be used to indicate the ability of this organism to prevent photobleaching of pigments under high light conditions.

Thorough sequencing of the mutated sites and characterization of the reconstructed site-directed mutants revealed that mutations required for the phototolerance are widely scattered over the randomly mutated locus (from Phe-180 to Ala-357) and that synergetic effects of the multiple mutations are necessary (*3*). Biochemical characterizations of these mutants did not show any rapid turnover or decreased degradation of D1 protein (Y. Narusaka, K. Satoh, M. Saeki, and H. Kobayashi, unpublished results), suggesting that the mechanism for phototolerance is not directly relevant to the so-called damage-repair cycle model (*6*). DNA sequencing of the recovered *psbA2* genes from the phototolerant mutants revealed that the mutation frequently occurs at the Asn-234 and Phe-260 positions in the D1 protein (Narusaka, Y., Satoh, K., Saeki, M., and Kobayashi, H., unpublished results). The NDFS mutant, which carries two mutations, N234D and F260S (Figure 1), was generated by site-directed mutagenesis based on this information (*3*). The former mutation locates near the end of the PEST-like region, which is postulated to be important for rapid turnover of D1 protein, and is therefore a primary target of mutagenesis in studies of D1 turnover (*7*−*8*). The F260S mutation locates in the latter half of the de-loop of D1 protein. Another mutant characterized in the present study, I6, one of the randomly generated phototolerant mutants, was determined to carry three mutations, S322I, I326F, and F328S, in the C-terminal loop exposed at the lumenal side (Figure 1). Throughout the present study, the mutants NDFS and I6 were used as representative phototolerant mutants at the acceptor and donor sides of PS II, respectively.

* Corresponding author: Telephone +81-48-462-1111, ext. 5543; Fax +81-48-462-4685; E-mail minagawa@postman.riken.go.jp.

‡ The Institute of Physical and Chemical Research.

§ Okayama University.

|| Present address: Laboratory of Fungicide Chemistry, National Institute of Agro-environmental Sciences, Tsukuba 305, Japan.

[1] Abbreviations: Chl, chlorophyll; DCMU, 3-(3,4-dichlorophenyl)-1,1-dimethylurea; E_m, redox midpoint potential; Ph, pheophytin; PS II, photosystem II; Q_A, primary acceptor plastoquinone; Q_B, secondary acceptor plastoquinone.

10.1021/bi981217x CCC: $18.00
Published on Web 12/22/1998

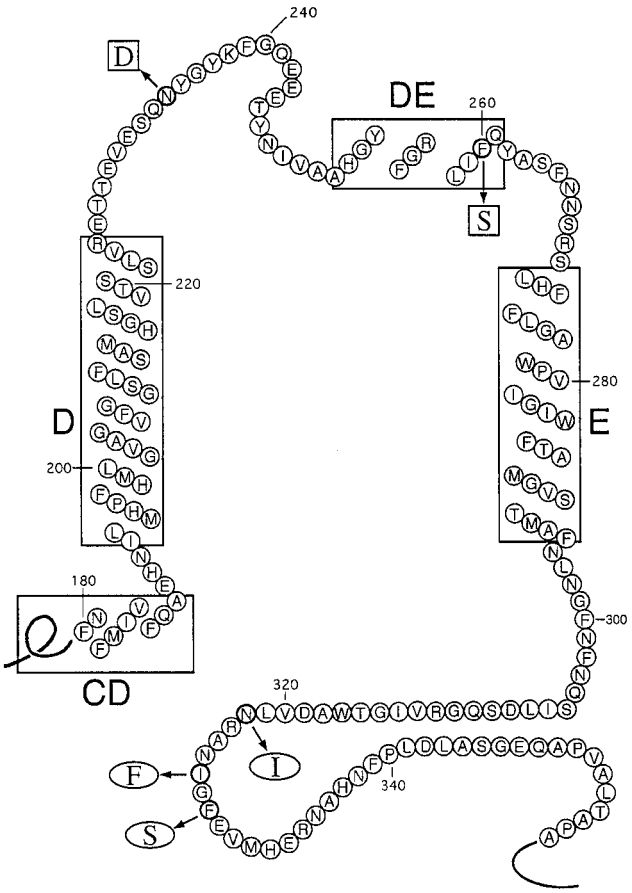

FIGURE 1: Location of the mutated residues on D1 protein of NDFS and I6 mutants. The positions in the ovals and squares display amino acid residues mutated in the I6 and NDFS mutants, respectively. Substitutions are indicated by arrows. D and E represent putative transmembrane helices.

Although we now know that these mutants afford increased resistance to pigment photobleaching, it is still not known whether there are any functional differences in the physiological properties of the PS II in these mutants that might underlie this dynamic process. In the present study, two phototolerant mutants, NDFS and I6, were analyzed by means of thermoluminescence measurements to monitor the thermodynamics of redox equivalents stored on the donor and acceptor sides of PS II. We discuss the expression mechanisms of phototolerance, or the nonphotobleaching phenotype, in these mutants. Possible implications, including decreased equilibrium constants for sharing an electron between the primary (Q_A) and secondary acceptor plastoquinones (Q_B), are also presented.

MATERIALS AND METHODS

(1) Strains and Growth Conditions. Mutants NDFS and I6 were constructed by random and site-directed mutagenesis, respectively, by transforming a *psbA1* and *psbA2* double deletion mutant, Cm4Δ-1 (ref *3*; Y. Narusaka, K. Satoh, M. Saeki, and H. Kobayashi, unpublished results). A nonmutagenized transformant with a kanamycin-resistance cassette (PC) was used as a wild-type control. *Synechocystis* sp. PCC 6803 strains were grown at 30 °C in BG-11 medium with continuous bubbling of air containing 3% CO_2. Cultures were irradiated with low light (white fluorescent bulbs, 50 μmol·m^{-2}·s^{-1}) or high light (heat-filtered halogen lamps, 500 μmol·m^{-2}·s^{-1}). Cultures in the logarithmic growth phase were routinely used for analysis by thermoluminescence measurements.

(2) Absorption Measurements. Optical absorption of the cells was measured with an MPS-2000 spectrophotometer (Shimadzu, Kyoto, Japan). Cell density was determined by optical density measurements at 750 nm in a cuvette with a 1 cm light path.

(3) Thermoluminescence Measurement. Thermoluminescence was measured essentially as described (*9*). Cyanobacterial cells (10 μg of Chl) were resuspended in 80 μL of fresh BG-11 medium with 5 mM Hepes/NaOH (pH 7.5) and 20% glycerol. We also used thylakoid membranes prepared as described (*8*) and obtained essentially the same results as those obtained by using living cell samples. To ensure a reproducible distribution of Q_B/Q_B^- and S_1/S_0 for all measurements, samples were preilluminated with continuous orange light for 30 s and dark-adapted at room temperature for 20 min. Actinic flashes were given by a xenon lamp at 5 °C (in the absence of DCMU) or at −10 °C (in the presence of 10 μM DCMU), followed by fast cooling in liquid nitrogen. Heating rate was maintained at 0.7 °C/s.

(4) Mathematical Analysis of Thermoluminescence Bands. A nonlinear least-squares curve-fitting of a single Randall−Wilkins band (*10*) to the main thermoluminescence band of the glow curves was performed with the software package IgorPro (Wavemetrics, Lake Oswego, OR). The free energy of detrapping (ΔF) at 25 °C was calculated from the activation energy and the frequency factor determined through curve-fitting. Equilibrium constants (K_{AB}) were calculated as described (*11*).

RESULTS

Growth Rate. The blue-green color of a wild-type *Synechocystis* culture is normally bleached upon exposure to high irradiance. Phototolerant mutants were separated from yellow-green colonies of nonmutagenized control cells under high irradiation (320 μmol·m^{-2}·s^{-1}). To examine if the color of the mutants or the wild-type strain was related to their viability, we first compared their growth rate under low (50 μmol·m^{-2}·s^{-1}) and high light (500 μmol·m^{-2}·s^{-1}) conditions. As shown in Figure 2A, the growth rates of the mutants and control cells were nearly identical under low light conditions. Mutant cells exposed to an irradiance of 500 μmol·m^{-2}·s^{-1} appeared to grow slightly faster in the late growth phase. Despite displaying a yellow-green color, wild-type cells exhibited a slightly faster growth rate in the earlier phase (Figure 2B). However, the differences in viability are not significant, even under high irradiance. When the cultures reached the stationary phase, they were diluted again and the light intensity was reduced to 50 μmol·m^{-2}·s^{-1}. After the transition, the two mutants and the wild-type cells immediately reinitiated propagation (Figure 2C), suggesting that photobleaching in wild-type cells did not reduce their viability. Consequently, it was inferred that the blue-green color of the mutants did not indicate that they are less susceptible (or more resistant) to photoinhibition than the wild-type cells but rather the mutants lack photosensitivity in some way that may be an important intrinsic control mechanism in wild-type cells.

Thermoluminescence upon Charge Recombination of $S_2Q_A^-$ and $S_2Q_B^-$ State. Given that the viability of the

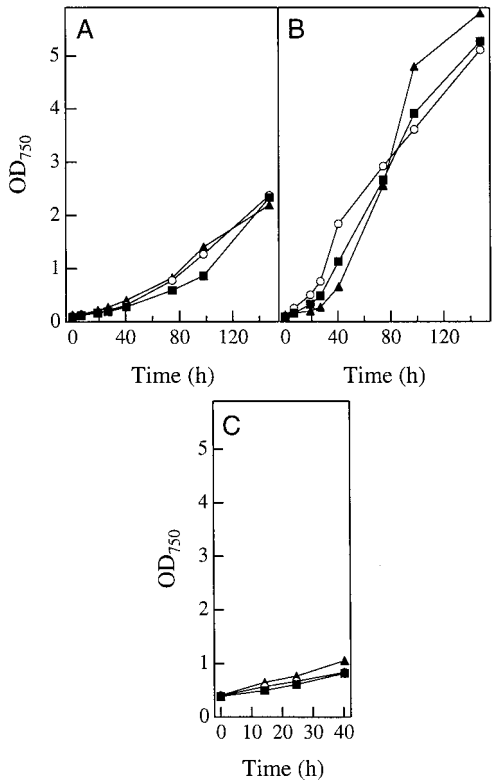

FIGURE 2: Growth curve of the mutants under illumination with low or high light. Cell densities were determined by measuring OD_{750} of cultures grown under illumination at 50 (panel *A*) or 500 μmol·m^{-2}·s^{-1} (panel *B*). After a 60 h exposure to high light intensity (500 μmol·m^{-2}·s^{-1}), cells were diluted and transferred to low light (panel *C*). I6 (▲), NDFS (■), and the wild-type control (○) are shown.

mutants was not significantly greater under high light conditions, a physiological study was undertaken to identify potential functional differences in PS II of the mutants. The blue-green color in the mutant cultures under high irradiance may be caused by modifications of PS II functions, since NDFS and I6 cells differ from wild-type cells only by mutations in the D1 protein sequences.

Thermoluminescence is the emission of light during rewarming of photosynthetic samples exposed to actinic illumination prior to freezing (for a recent review, see ref *12*). In the experiments described here, thermoluminescence is due to thermally stimulated recombination of pairs of opposite charges generated by light-induced charge separation in the PS II complex. Thermoluminescence emission peaked at approximately 35 °C (B-band) results largely from the recombination of the $S_2Q_B^-$ charge pair. At around 10 °C, the addition of DCMU to the sample, which blocks oxidation of Q_A^- by Q_B, induces a major emission component (Q-band) from $S_2Q_A^-$ recombination. The peak temperature of a thermoluminescence component is indicative of the energetic stability of a separated charge pair. As a general rule, the higher the peak temperature, the greater the stabilization.

Figure 3 shows the glow curves of the wild-type and mutant cells that were illuminated with a single-turnover flash in the presence (curves **a**−**c**) or absence (curves **d**−**f**) of DCMU. A markedly different behavior of the B-band is observed in the NDFS mutant. Emission temperature of the B-band was shifted down by 8 °C compared to the wild type.

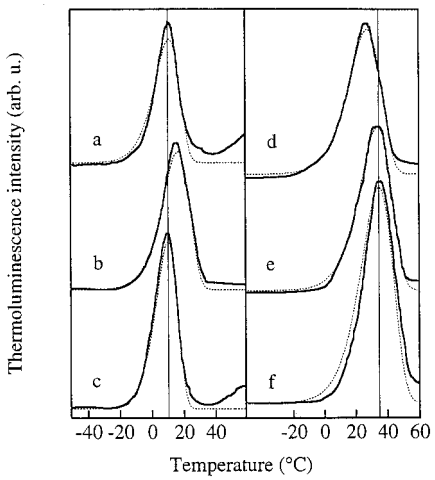

FIGURE 3: Thermoluminescence glow curves. Glow curves of DCMU-treated (solid curves a−c) and untreated cells (solid curves d−f) and theoretical Randall−Wilkins curves (broken curves) are shown. Cells resuspended in a fresh BG-11 medium with 5 mM Hepes/NaOH (pH 7.5) and 20% glycerol were excited by a single flash at −10 °C for DCMU- (10 μM) treated samples or at 5 °C for untreated samples after dark adaptation. NDFS mutants (a, d), I6 mutants (b, e), and the wild-type controls (c, f) are shown.

This indicates that the energetic stability of the $S_2Q_B^-$ charge pair was decreased in the NDFS mutant. In contrast, the position of the Q-band was essentially the same as in the wild-type cells, showing that the stability of the $S_2Q_A^-$ charge pair is the same as that of the wild type. The temperature at which maximal luminescence occurs is a function of the free energy of stabilization of the charge-separated state, which depends on the depth of the traps for electrons and holes (*10*−*12*). The B-band reflects the free energy gap between the redox couples Q_B/Q_B^- and S_2/S_1. Since the S_2 state is a common recombination partner in the two charge pairs ($S_2Q_A^-$ and $S_2Q_B^-$), it is more likely that the effect of the NDFS mutation is limited to the modified redox potential (E_m) of the Q_B/Q_B^- redox couple. In general, a downshifted thermoluminescence band results from shallower depths of the traps for a recombination partner. Accordingly, a downshifted B-band in the NDFS mutant could be due to the lowered E_m of the Q_B/Q_B^- couple.

The donor-side I6 mutant exhibited an increase in emission temperature of the Q-band by 6 °C, although the B-band was normal. This indicates that the stability of the $S_2Q_A^-$ charge pair increased, whereas the $S_2Q_B^-$ charge pair was unchanged. A shifted Q-band could be accounted for by a modified E_m of the reduced plastoquinone at the Q_A site, although it is also possible that a lowered E_m of S_2/S_1 upshifts the Q-band. If the latter is true, the E_m of both S_2/S_1 and Q_B/Q_B^- couples should decrease simultaneously to a similar extent, such that the emission temperature of the B-band is not changed. Alternatively, the change may arise as a result of a higher E_m of the Q_A/Q_A^- couple in the I6 mutant.

Since the NDFS mutant has a Q_B/Q_B^- couple of lower E_m and the I6 mutant has a Q_A/Q_A^- couple of higher E_m, the redox gap between the two redox couples Q_A/Q_A^- and Q_B/Q_B^-, appears to decrease in both mutants, resulting in smaller equilibrium constants for the electron-transfer reaction between Q_A^- and Q_B. Estimation of the equilibrium constants based on the proposed theory of thermoluminescence (*10*) will be discussed in the Discussion section.

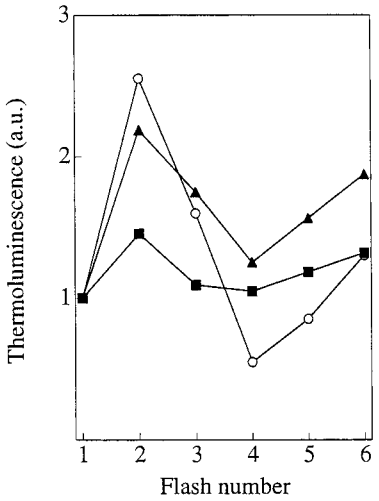

FIGURE 4: Oscillation of B-band thermoluminescence. Heights of B-band thermoluminescence from I6 (▲), NDFS (■), and the wild-type control (○) were plotted as a function of the number of flashes given prior to measurements. B-band heights on the first flash of the mutants were normalized to that of the wild type.

Oscillation of Thermoluminescence B-Band Intensity. Further information may be obtained by analyzing the thermoluminescence yield as a function of flash number upon illumination of dark-adapted samples with a series of short saturating flashes. When excited by a series of saturating flashes, the intensity of the B-band exhibits a period four oscillation (*13*). The oscillation is caused by different populations of S_2 and S_3, the binary oscillation of the acceptor side, and the different quantum yields of excited singlet-state formation at P_{680} due to detrapping of holes and electrons from these states (*14*).

Figure 4 shows that the wild-type cells exhibit a typical period four oscillation. A markedly damped B-band oscillatory pattern is observed in the mutants. The oscillatory pattern in the I6 mutant exhibited a slightly damped period four oscillation compared to the wild-type cells. The acceptor-side NDFS mutant exhibited even greater damping. The ratios of thermoluminescence emission after one and two flashes were 2.2, 1.4, and 2.6 in the I6 mutants, NDFS cells, and the wild-type cells, respectively. The damping is most likely caused by an increased probability of error at the acceptor and/or donor side or a decreased S_1 concentration in the mutants.

DISCUSSION

In this study, simultaneous mutations in the acceptor side, N234D and F260S (NDFS mutant), and in the donor side, S322I, I326F, and F328S (I6 mutant), in *Synechosystis* sp. PCC 6803, were shown not to have drastic effects on their growth rates. To elucidate the molecular mechanism for their insensitivity to photobleaching, the functional significance of mutations in PS II photochemistry was studied by thermoluminescence measurements. We found that these mutations have marked effects on the function of PS II as reflected by (a) a downshifted B-band in the NDFS mutant, (b) an upshifted Q-band in the I6 mutant, and (c) increased damping of the period four oscillations of the B-band.

The downshifted thermoluminescence B-band observed in the acceptor-side NDFS mutant could be accounted for by a decrease in E_m of the Q_B/Q_B^- redox couple. The intensity of B-band oscillation after exposure to a series of actinic flashes was significantly damped compared to the wild type. Analogous phenomena have been observed in herbicide-resistant mutants of many species (*15*−*19*) and a site-specific deletion of the PEST-like region in cyanobacteria (*8*). These results can be explained by the assumption that mutations in the vicinity of the Q_B site cause a thermodynamic destabilization of the semiquinone form of the plastoquinone noncovalently bound to the site. This effect leads to (i) a lowering of the trap depth for electrons stored at Q_B^-, thereby giving rise to a decreased thermoluminescence peak temperature of the B-band, and to (ii) a shift of the redox equilibrium $Q_A^-Q_B \leftrightarrow Q_AQ_B^-$ toward $Q_A^-Q_B$, which causes an increased probability of misses and therefore a damping of the oscillation pattern.

Table 1: Thermoluminescence Characteristics and Equilibrium Constant of Q_A and Q_B[a]

strain	designation of bands	T_m (°C)	ΔF(25 °C) (eV)	K_{AB}
control				
	B (no addition)	36	0.849	26
	Q (+DCMU)	10	0.765	
I6				
	B (no addition)	35	0.843	8
	Q (+DCMU)	16	0.791	
NDFS				
	B (no addition)	28	0.827	9
	Q (+DCMU)	10	0.770	

[a] Characteristics of the thermoluminescence bands, shown in Figure 3, were obtained by a nonlinear least-squares fitting of the glow curves (*10*). Equilibrium constants were calculated by assuming that the redox properties in the donor side were not modified in the mutants. T_m, peak temperature of a thermoluminescence band; ΔF, free energy of detrapping; K_{AB}, equilibrium constant of the primary (Q_A) and secondary (Q_B) acceptor plastoquinones.

Model-based calculations of free energy of detrapping for a photosynthetic thermoluminescence band have been proposed by several groups (for a recent review, see ref *20*). These works were basically a generalization of a simple model for thermoluminescence from solid states, which was first developed by Randall and Wilkins (*21*). Since the multistep recombination from a pair of oxidized donor and reduced acceptor in PS II was simply treated as a single-step process, we should note the limitations of these previous attempts. Nevertheless, as this approach resulted in good predictions for the stabilization free energies (*20*), it should be worthwhile to predict free energies of detrapping for the thermoluminescence bands in the phototolerant mutants and the wild-type control by one of these methods (*10*) and estimate to what extent the equilibrium constants for sharing an electron between Q_A and Q_B in the mutants were modified. The predicted values are shown in Table 1. By comparing the free energies of detrapping obtained for the B-bands with those of the control, the extent of the shift in the E_m of the Q_B/Q_B^- couple in the NDFS mutant was estimated (22 mV). The redox distances between Q_A and Q_B in the NDFS mutant and the wild type were 57 and 83 mV, respectively. The E_m shift could result in either retardation of the forward electron-transfer rate from Q_A^- to Q_B or acceleration of the reverse reaction from Q_B^- to Q_A, or a combination of these effects. On the basis of measurements of the relaxation kinetics of flash-induced fluorescence quantum yield changes (J. Minagawa, Y. Narusaka, Y. Inoue, and K. Satoh, unpublished results), the initial rate of Q_A^- reoxidation by Q_B remained

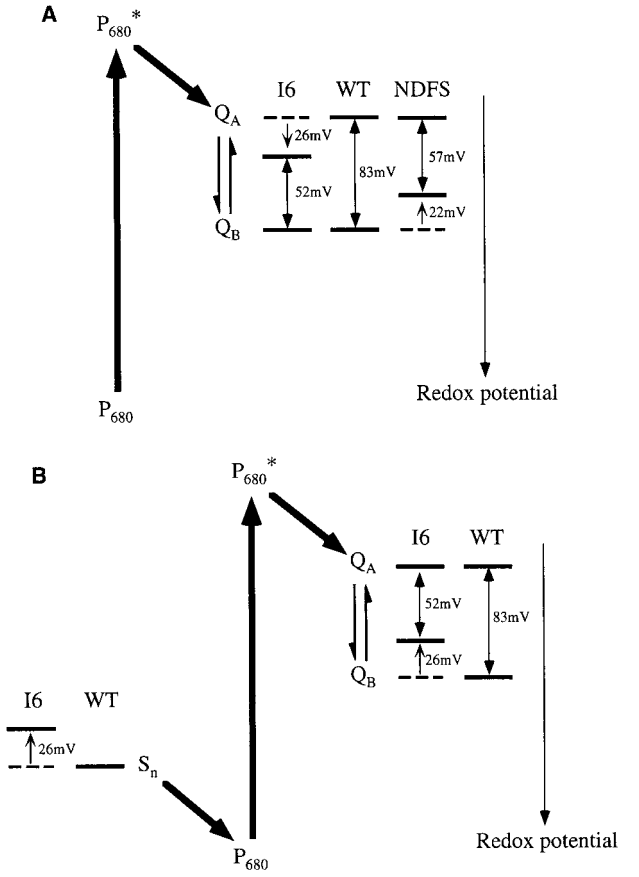

FIGURE 5: Models for the redox properties of PS II in the mutants. On the basis of the results obtained in this study, two possible models are shown. Model A is based upon the assumption that redox properties of the donor-side components were not modified in the mutants. Model B reflects observations for the I6 mutants wherein the upshift of the Q-band is induced by modifications in the donor side.

virtually unchanged. Therefore, the reverse electron transfer from Q_B^- to Q_A must be accelerated. Regardless of these mechanistic details, the shift of peak temperature permits estimation of the E_m shift of Q_B/Q_B^-, provided that the energetics of the holes in the donor-side traps remain unmodified.

The emission temperature of Q-band of the donor-side I6 mutant increased by 6 °C in thermoluminescence measurements, although the B-band was virtually unchanged. Since a shift in thermoluminescence peak temperature can similarly result from the influences on either the donor or acceptor sides, the following alternatives must be considered when interpreting the selective effect on the Q-band. The mutations in the I6 mutant specifically modified (i) the E_m of the Q_A/Q_A^- couple without affecting that of the Q_B/Q_B^- or S_2/S_1 couple (Figure 5, model A), or (ii) the E_m of both Q_B/Q_B^- and S_2/S_1 couples with negligible influence on the Q_A/Q_A^- couple, provided that changes in E_m of Q_B/Q_B^- and S_2/S_1 negate each other to result in a virtually unaffected B-band (Figure 5, model B). This situation is akin to that observed upon removal of the 33K extrinsic protein from PS II in vitro (*22*) or in the measurements of the *psbO*-deficient mutant of *Synechocystis* sp. PCC 6803 (*23*). Since mutations in the I6 mutant are located on the donor side (Figure 1) and the role of the 33K protein in Mn-complex stabilization is well established, modifications of the donor-side redox properties represent a more likely scenario. In fact, a mutant lacking the lumen-exposed loop of the internal antenna protein CP47 demonstrated that both Q- and B-bands were upshifted (*24*), which could simply suggest a lowered E_m of the S_2/S_1 couple in these donor-side mutants. However, if we assume that modulation of E_m of S_2/S_1 explains the upshifted Q-band observed in the I6 mutant, we should also assume modulation of E_m of Q_B/Q_B^-, which exerts a compensatory effect on the $S_2Q_B^-$ charge recombination, resulting in no apparent shift on the B-band. If one could question the possibility of transmembrane modulation of the Q_A site (model A), the possibility of modification of the Q_B site (model B) would also need to be addressed. In either case, the donor-side mutations in the I6 mutant seem to induce a transmembrane effect to the acceptor side. Further studies, such as a direct determination of the E_m of the Q_A/Q_A^- couple, will provide more insight on this issue.

It should be noted, however, there have been several recent reports of donor-side-induced shifts in the redox properties of the primary acceptor plastoquinone. The E_m of the Q_A/Q_A^- couple in the active PS II center was 190 mV lower than that of the center prior to photoactivation of the Mn cluster in PS II (*25*), and it increased from −80 mV to +65 mV upon Ca depletion (*26*). On the basis of these results, Rutherford and his colleagues proposed that the increase in E_m of Q_A/Q_A^- results in a protection of the reaction center from light damage by changing the dominant charge recombination pathway to one that does not involve the formation of a $P_{680}^+Ph^-$ radical pair, which decreases the yield of P_{680} triplet and singlet oxygen (*25*, *27*). Assuming that the redox properties in the donor side were not modified so that the shift of Q-band can only be ascribed to a modulation of the Q_A/Q_A^- couple, the extent of the increase in E_m of the Q_A/Q_A^- couple in the I6 mutant is estimated to be about 26 mV, which reduces the redox distance between Q_A and Q_B to 52 mV (Table 1).

The present results suggest that the electron transfer from Q_A^- to Q_B is perturbed, which results in inefficient electron transfer through PS II. Two possible models explain how the modified redox properties of PS II in the mutants perturb electron transfer (Figure 5**)**. If the downshifted B-band in the NDFS mutant and the upshifted Q-band in the I6 mutant were due to the decrease in the E_m of Q_B/Q_B^- and an increase in the E_m of Q_A/Q_A^-, respectively, the redox gaps between the primary and secondary acceptor plastoquinones in both of the mutants become smaller. This inhibits electron transfer from Q_A^- to Q_B due to a decrease in the equilibrium constant for the reaction $Q_A^-\ Q_B \leftrightarrow Q_A\ Q_B^-$ (Figure 5, model A). The equilibrium constant for this reaction (K_{AB}) can be calculated by using the redox distance between Q_A and Q_B as estimated by the Randall−Wilkins-type simulation of the thermoluminescence bands (Table 1). Although a value of $K_{AB} = 26$ was obtained for the wild-type, due to the modification of redox properties of Q_A/Q_A^- and Q_B/Q_B^-, K_{AB} for the I6 and NDFS mutants were only 8 and 9, respectively. Care should be taken in assessing this model, since thermoluminescence measurements alone do not permit an unambiguous separation of donor- and acceptor-side effects. Interestingly, however, the redox gap between Q_A/Q_A^- and Q_B/Q_B^- should also be smaller in case the upshift of the Q-band in the I6 mutant is induced by modulation of E_m of both Q_B/Q_B^- and S_2/S_1 couples with negligible influence on

the Q_A/Q_A^- couple, provided that changes in E_m of Q_B/Q_B^- and S_2/S_1 approximately compensate for each other to result in a virtually unaffected B-band (Figure 5, model B). In either case, we conclude that electron transfer between Q_A and Q_B is thermodynamically perturbed in both I6 and NDFS mutants. Indeed, analysis of light-response curves for photochemical quenching (q_P) for these mutants reveals the smaller proportion of open PS II centers in the mutants and supports the perturbed electron transfer between Q_A and Q_B (J. Minagawa, Y. Narusaka, Y. Inoue, and K. Satoh, unpublished results).

Since the two mutants, NDFS and I6, were almost indistinguishable in color, there may exist a common mechanism for their ability to form blue-green colonies under high irradiance. It is then hypothesized that inefficient electron flow through PS II in the two mutants, NDFS and I6, does not give a cue to a signal transduction for changing the pigment composition to adapt to high light. The amino acid displacements in the phototolerant mutants appear to be randomly distributed over the entire region affected by in vitro mutagenesis (*5*). If the above hypothesis is correct, the random distribution also might be understandable, as it is hard to believe that so many different residues could contribute to make an elaborate biological function more efficient. The current PS II complex is probably the most efficient machinery for photochemistry that is a product of a long evolutionary process.

ACKNOWLEDGMENT

We thank Drs. Sandor Demeter and Imre Vass for their valuable discussion.

REFERENCES

1. Satoh, K. (1996) in *Oxygenic Photosynthesis: The Light Reactions* (Ort, D. R., and Yocum, C. F., Eds.) pp 193−211, Kluwer Academic Publishers, Dordrecht, The Netherlands.
2. Barber, J., and Andersson, B. (1992) *Trends Biochem. Sci. 17*, 61−66.
3. Narusaka, Y., Saeki, M., Kobayashi, H., and Satoh, K. (1995) in *Photosynthesis: from Light to Biosphere* (Mathis, P., Ed.) Vol. IV, pp 235−238, Kluwer Academic Publishers, Dordrecht, The Netherlands.
4. Narusaka, Y., Murakami, A., Saeki, J., Kobayashi, H., and Satoh, K. (1996) *Plant Sci. 115*, 261−266.
5. Satoh K. (1998) in *Stress Responses of Photosynthetic Organisms* (Satoh, K., and Murata, N., Eds.) pp 3−14, Elsevier, Amsterdam, The Netherlands.
6. Ohad, I., Kyle, D. J., and Arntzen, C. J. (1984) *J. Cell Biol. 99*, 481−485.
7. Mäenpää, P., Kallio, T., Mulo, P., Salih, G., Aro, E.-M., Tyystjärvi, E., and Jansson, C. (1993) *Plant Mol. Biol. 22*, 1−12.
8. Nixon, P. J., Komenda, J., Barber, J., Deak, Z., Vass, I., and Diner, B. A. (1995) *J. Biol. Chem. 270*, 14919−14927.
9. Ono, T.-A., and Inoue, Y. (1986) *Biochim. Biophys. Acta 850*, 380−389.
10. Vass, I., Horváth, G., Herczeg, T., and Demeter, S. (1981) *Biochim. Biophys. Acta 634*, 140−152.
11. DeVault, D., Govindjee, and Arnold, W. (1983) *Proc. Natl. Acad. Sci. U.S.A. 80*, 983−987.
12. Inoue, Y. (1996) in *Biophysical Techniques in Photosynthesis* (Amez, J., and Hoff, A. J., Eds.) pp 93−107, Kluwer Academic Publishers, Dordrecht, The Netherlands.
13. Inoue, Y., and Shibata, K. (1977) *FEBS Lett. 85*, 193−197.
14. Rutherford, A. W., Crofts, A. R., and Inoue, Y. (1982) *Biochim. Biophys. Acta 682*, 457−465.
15. Demeter, S., Vass, I., Hideg, E., and Sallai, A. (1985) *Biochim. Biophys. Acta 806*, 16−24.
16. Etienne, A.-L., Ducruet, J.-M., Ajlani, G., and Vernotte, C. (1990) *Biochim. Biophys. Acta 1015*, 435−440.
17. Gleiter, H. M., Ohad, N., Hirschberg, J., Fromme, R., Renger, G., Koike, H., and Inoue, Y. (1990) *Z. Naturforsch. 45c*, 353−358.
18. Ohad, N., Amir-Shapira, D., Koike, H., Inoue, Y., Ohad, I., and Hirschberg, J. (1990) *Z. Naturforsch. 45c*, 402−407.
19. Gleiter, H. M., Ohad, N., Koike, H., Hirschberg, J., Renger, G., and Inoue, Y. (1992) *Biochim. Biophys. Acta 1140*, 135−143.
20. Vass, I., and Govindjee (1996) *Photosynth. Res. 48*, 117−126.
21. Randall, J. T., and Wilkins, M. H. F. (1945) *Proc. R. Soc. London A 184*, 366−369.
22. Vass, I., Ono, T.-A., and Inoue, Y. (1987) *FEBS Lett. 211*, 215−220.
23. Vass, I., Cook, K. M., Deák, Z., Mayes, S. R., and Barber, J. (1992) *Biochim. Biophys Acta 1102*, 195−201.
24. Gleiter, H. M., Haag, E., Shen, J.-R., Eaton-Rye, J. J., Inoue, Y., Vermaas, W. F. J., and Renger, G. (1994) *Biochemistry 33*, 12063−12071.
25. Johnson, G. N., Rutherford, A. W., and Krieger, A. (1995) *Biochim. Biophys. Acta 1229*, 202−207.
26. Krieger, A., Rutherford, A. W., and Johnson, G. N. (1995) *Biochim. Biophys. Acta 1229*, 193−201.
27. Krieger, A., and Rutherford, A. W. (1997) *Biochim. Biophys. Acta 1319*, 91−98.

BI981217X